A unified multiple stress reliability model for microelectronic devices - Application to 1.55 μm DFB laser diode module for space validation

Alain Bensoussan, Ephraim Suhir, Philip Henderson, Mustapha Zahir

A unified multiple stress reliability model for microelectronic devices — Application to 1.55 μm DFB laser diode module for space validation

A. Bensoussan [a,b,*], E. Suhir [c,d,e], P. Henderson [f], M. Zahir [g]

[a] Institut de Recherche Technologique Saint Exupery, 31432 Toulouse, France
[b] Thales Alenia Space France, 31037 Toulouse, France
[c] Portland State University, Portland, OR, USA
[d] Technical University, Vienna, Austria
[e] ERS Co., Los Altos, CA, USA
[f] Gooch & Housego, Torkay, Devon TQ2 7QY, United Kingdom
[g] European Space Agency ESTEC, Noordwijk, The Netherlands

A B S T R A C T

The establishment of European suppliers for DFB Laser Modules at 1.55 μm is considered to be essential in the context of future European space programs, where availability, cost and schedule are of primary concerns. Also, in order to minimize the risk, associated with such a development, the supplier will be requested to use components which have already been evaluated and/or validated and/or qualified for space applications. The Arrhenius model is an empirical equation able to model temperature acceleration failure modes and failure mechanisms. The Eyring model is a general representation of Arrhenius equation which takes into account additional stresses than temperature. The present paper suggests to take advantage of these existing theories and derives a unified multiple stress reliability model for electronic devices in order to quantify and predict their reliability figures when operating under multiple stress in harsh environment as for Aerospace, Space, Nuclear, Submarine, Transport or Ground. Application to DFB laser diode module technologies is analyzed and discussed based on evaluation test program under implementation.

DFB laser diode
Optopelectronics
Reliability
Design-for-Reliability

1. Introduction

State-of-the-art Distributed FeedBack (DFB) laser modules integrated with a photodiode monitor provide excellent long-term wavelength stability. By adopting unique and compact configuration, wavelength deviations of as small as a few picometers have been achieved. The laser modules are improved also in the scope of high power, high reliability, and wavelength tunability. Available reliability test results of DFB laser diodes and modules indicate that a sufficiently long lifetime and a small wavelength drift are possible. However, a space validation of this type of lasers has not been performed at the required wavelength of 1.55 μm. Due to the potential applications for the DFB Lasers, including Intra and Inter-satellite communication, a space validation is now required. This activity is part of the European Component Initiative program funded by European Space Agency. The objectives are to design, develop, manufacture and space validate a DFB Laser Module at 1.55 μm manufactured by a European supplier. Although the space validation exercise in progress is performed according to the ECSS-ST-60-05-Rev1, where the LAT (Lot Acceptance Test) will be replaced by an Evaluation program based on the new Evaluation Test program (ETP) for Laser Diode guideline. A part of the study have been conducted to consolidate and apply a unified multiple stress reliability model defined for microelectronic devices and to be published soon. The definition of maximum rating and derating parameters are extracted and justified thanks to the model presented. Reliability figures including activation energies and accelerating factors related to the three main parameters will be commented (temperature, current and optical stress). It will be shown how these multiple stresses will interact and modify the effective activation energy. Additional evaluation step stress program is suggested to consolidate and validate the model.

The paper presents a generalized view of the existing reliability models and shows reliability mathematic formulas. In 2013 Ref. [3,4] have presented two advanced Probabilistic Design-for-Reliability (PDfR) concepts to address the prediction of the reliability of aerospace electronics: 1) Boltzmann–Arrhenius–Zhurkov (BAZ) model for the evaluation of the probability of failure (ProF) after the given time in operation at the given temperature and under the given stress (not necessarily mechanical), and 2) extreme value distribution (EVD) technique that can be used to predict the number of repetitive loadings that closes the gap between the capacity (stress-free activation energy) of a material (device) and the demand (loading), thereby leading to a failure.

* Corresponding author. Thales Alenia Space France, 31037 Toulouse, France.

The BAZ model determines the lifetime τ for a material or a device experiencing combined action of an elevated temperature and external stress

$$\tau = \tau_0 \cdot \exp\frac{(U_0 - \gamma \cdot S)}{k \cdot T} \tag{1}$$

where S is the applied stress, T is the absolute temperature that could be as a function of the applied stress S, τ_0 is the time constant, γ is a factor of loading characterizing the role of the level of stress (the product $\gamma \cdot S$ is the stress per unit volume and is measured in the same units as the activation energy U_0), and k the Boltzmann's constant (1.3807 10^{-23} J/K or 8.6174 10^{-5} eV/K).

The effect of temperature on electronic devices is often estimated by extrapolating from accelerated tests at extremely high temperatures: this is not always possible. Particularly when stress induced failures are driven by non-thermal constraints as for example static and dynamic electrical stresses, the accelerating factor is interdependent and related. It is the case for DFB laser diode module which is designed with internal temperature control based on Thermoelectric Cooler. Consequently, conducting accelerated high temperature testing is quite limited. Nevertheless, electrical and cumulated output power light under multiple stresses may bring adequate accelerating factor able to accelerate a failure mechanism. From the forest of existing models it is observed the well-known Arrhenius law applies with some corrective factors as for example observed for the Black law, Coffin–Manson or Eyring law, effect of humidity or the hydrogen poisoning effect in semiconductors. Is it possible to harmonize these facts for so large range of reliability figures of well stabilized technologies?

A unified reliability model can be assessed but will have to consider de facto an effective activation energy as already suggested by the BAZ model which takes into account healthiness of the product, biasing condition derated from Safe Operating Area and any extrinsic stress applied to the device during life operation.

The paradigm of the Transition State Theory (TST) [1,2] developed by E. Wigner in 1934 [11] and by M. Evans, M. Polanyi in 1938 [12] is viewed as an equivalent approach to the BAZ model.

2. Transition state theory applied to reliability and physics of failure

Reliability investigations reported in various books and tutorials have been synthesized as for example on the Reliability of GaAs MMICs book edited by A. Christou [13].

Reliability models (Electromigration [5,7], Ohmic contact degradation [25,26], Coffin–Manson model [14], Eyring model [6,23,24], Humidity model [8], TDDB [15,16], Hot Carrier Injection [17,18], Hydrogen poisoning [9,19-21], Thermo-mechanical stress [22], NBTI [23], etc…) are generally expressed by a function of stress parameter multiplying the exponential activation energy factor [10]. These expressions may not look much like a multiple-stress model but in fact it is as we have shown in paper presented at the 2013 IEEE Aerospace Conference [4]:

$$\tau = \tau_0 \cdot f(\chi) \cdot \exp\frac{E_a}{k \cdot T}. \tag{2}$$

Writing $f(S) = \exp(\log(f(\chi))$, Eq. (1) reduces to:

$$\tau = \tau_0 \cdot \exp\frac{Ea + \log(f(\chi))}{k \cdot T} = \tau_0 \cdot \exp\frac{E_{a\_effective}}{k \cdot T}. \tag{3}$$

Let's write differently Eq. (3) and take into consideration normalized stressors w.r.t. their maximum rating limits. The $f(\chi)$ relation modeling the function stress factors for $i = 1$ to M, is generalized and rewritten being equivalent to

$$f(\chi_i) = \gamma_i \cdot S_i^{m_i} = e^{\nu_i \cdot \left(S_{i_{burnout}} \cdot \chi_i\right)} \tag{4.a}$$

$$\text{or} \qquad f(\chi_i) = e^{(\gamma_i \cdot S_i)} = e^{\gamma_i \cdot S_{i_{burnout}} \cdot \chi_i} \tag{4.b}$$

m_i the power law factors and γ_i are constants, all to be determined experimentally.

Considering expression 4.a relates to electromigration (gate sinking or ohmic contact degradation), corrosion (Power law model), Hot Carrier Injection, surface inversion (mobile ions), temperature cycling and thermal shocks, mechanical stress migration Hydrogen poisoning, and Power slump (not exhaustively). Expression 4.b relates to TDDB, corrosion (exponential law), Negative Bias Temperature Instability.

Rewriting 3 and bearing in mind a number of stress conditions from $i = 1$ to M and $j = 1$ to N, we can resume:

$$\tau = \tau_0 \cdot \exp\frac{E_a \cdot c\left(\chi_{i,j}\right)}{k \cdot T_{eff}} \tag{5}$$

with

$$c\left(\chi_{i,j}\right) = 1 + \frac{k.T_{eff}}{E_a} \cdot \left[\sum_{i=1}^{M}\left(\nu_i \cdot S_{i_{burnout}} \cdot \chi_i\right) + \sum_{j=1}^{N}\left(\gamma_j \cdot S_{j_{burnout}} \cdot \chi_j\right)\right] \tag{6}$$

where $S_{i,j\_burnout}$ are the corresponding maximum catastrophic burnout failure limits related to measurement of each electrical stress parameter, T_{eff} is the absolute temperature that could be a function of the applied stress $\chi_{i,j}$ when joule effect is occurring, τ_0 is the time constant, ν_i and γ_i are the factors of loading characterizing the weight of the level of stresses and k the Boltzmann's constant.

The stress load factor $c(\chi_{i,j})$ (for any i or j) is seen as equal to 1 when no stress is operated or equal to 0 when stress burnout is applied (modeling the consequence of sudden catastrophic failure with an effective activation energy equal to 0). Note the stress burnout level is related either to a single stress condition or modified when a set of stress condition combination is applied simultaneously to the device as they can act in synergy and cause catastrophic burnout in an accumulative process. That's the reason why defining single burnout limit can be particularly sensitive and questionable. Because of the stress load factor $c(\chi_{i,j})$ is comprised between 0 and 1, the ν's and γ's can be calculated when applying boundary conditions achieved when measuring the level of overstress burnout limits considering statistical distribution parameters. The numerical example is detailed at the end of this paper in the paragraph related to the laser diode module. As a consequence the stress load $c(\chi_{i,j})$ must also be considered as a factor with similar statistical distribution behavior. In the following paragraph, the transition State Theory model will give more physical description of this factor and the related comments.

Eq. (6) helps to unify the model because the term $c(\chi_{i,j})$ is now a parameter which is in the range [0, 1] as in one hand, we can't have $c(\chi_{i,j}) < 0$ by definition because the effective activation energy must be a positive term and in other hand we can't exceed Ea given by the Arrhenius activation energy due to pure diffusion mechanism. Formerly, Transition-State Theory [1] could be used to model the Probabilistic Design for Reliability (PDfR) concept developed for electronics devices in harsh environment.

Fig. 1 shows a schematic drawing of the principle of the Transition State Theory which represents the amount of energy $\Delta G^{\ddagger}$ required to allow a chemical reaction to occur from an initial state to a final state. If the chemical reaction is accelerated by a catalyst effect the height of energy $\Delta G^{\ddagger}$ is reduced allowing the transition Initial state → Final State to occur with less energy brought to the system at initial state.

Similarly in Reliability domain, when considering reliability figures of electronic devices or products, a reaction occurs during aging and stress of these devices (Initial State = healthy devices, and Final State = failed devices). The reaction is accelerated by both the temperature and the stresses applied to the devices considered as catalyst processes: it is important to note that the temperature is a factor which defines the quantification of the energy and influences the

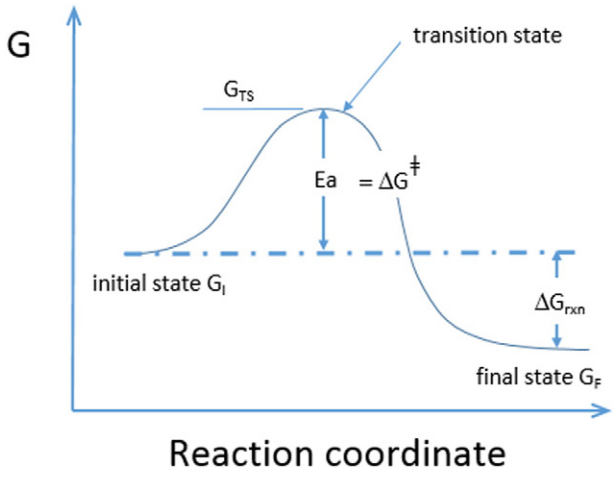

Fig. 1. Transition State Theory principle.

transition rate through the Arrhenius factor exp[Ea/kT] while other stress factors χ are impacting the height of the transition state.

Assuming the internal free energy, G_I, represents the internal energy of a device i.e. reflecting a kind of measurement of the healthiness of a device. The more the free energy G_I is close to the highest point of the free energy diagram (the transition state energy) the more the device is considered pre-damaged. When such a device has its free energy equal to the transition state energy, the probability to fall down to final state F is equal to 1. At this state, the device can suddenly drop down into the final state G_F then be considered as failed. The emphasis is on the application of the powerful and flexible Boltzmann–Arrhenius–Zhurkov (BAZ) model [27], and particularly on its multi-parametric aspect.

Fig. 1 details the equivalent concept we can consider: assuming final state is related to the free energy of any failed device (a single state) and initial states relate to the level of free energy of each individual healthy product (component or electronic device) at initial time i.e. just after production release. The transition state G_{TS} represents the point of highest free energy for a reaction step to be effective. The initial state (respectively final state) is represented by free energy G_I (respectively G_F) in the Gibbs free energy diagram.

The transition step applied on healthy devices to failed devices is activated by temperature and time in order to overpass the barrier of energy of the intermediate transition state by an amount of E_a (the activation energy). When superimposing stress condition other than temperature to a device, the result is to reduce the height of the energy state. Similarly, voltage stress or any other type of stressor (including radiation) will reduce the rate of transition from initial to final state but will reduce the level of the transition state by an amount proportional to the stress applied.

Arrhenius equation applied to chemical reaction relates the reaction rate R to temperature is:

$$R = \frac{1}{\tau} \propto \exp\left(-\frac{E_{a\_effective}}{k \cdot T}\right). \tag{7}$$

The equivalence with Transition State Theory is supported by the fact that the transition rate is similarly outlined by Eq. (1) of BAZ model when a catalyst effect is invoked.

3. Reliability model of 1550 nm DFB laser diode module

Laser-based free-space communication systems are attractive contenders when high-rate data are to be transmitted. A 10 GHz/100 mW European space-qualified product, future development of 1.55 μm DFB laser module is likely to see significant advances in modulation rate and power. For operation on-board a satellite, there are several additional requirements that must be considered or which have to be accentuated. Special design solutions may be necessary to cope with that. Commercial designs are based around the requirements of Telcordia GR-468 CORE which in turn is based upon MIL-STD 883. This qualification protocol is used for the telecommunications industry and is aimed at setting a very high level of quality and reliability for that industry. Submarine deployment of telecommunications comes closest to the ultrahigh reliability requirements of space deployment in that recovery and repair of failed undersea systems is extremely expensive placing a very large premium on reliability. However, even this regime does not address many of the concerns of space applications.

Avionic and other military applications can have very demanding environmental requirements such as mechanical shock and vibration, operating temperature range and operation over a wide range of atmospheric pressures. The following numerical application is based on a laser specifically developed for wavelength division multiplexing (WDM) systems, where it is used as a wavelength selected source in combination with an external modulator, such as the LiNbO3-based Mach–Zehnder. The specifications of a representative 50 mW 1.55 μm CW DFB Lasers with PM Fiber for WDM Applications developed by a Manufacturer M are listed in Table 1. Maximum rating parameters are also defined for such laser diode including forward current bias and radiant output power from pigtail.

These two parameters are plotted in Fig. 2 and assumed to be the stressor parameters as shown linked by the following relation:

$$P_{output} = \eta_D \cdot (I - I_{th}). \tag{8}$$

Fig. 2 shows how the derating parameters applied to the stressors are impacted by the Quantum Efficiency parameter as distributed around the mean value for a considered manufacturing lot. The derating limits are observed to be defined by the most stringent conditions either applied to operating current or to output power parameter (whichever is first achieved for 50% P_{max_rating} or 75% I_{max_rating}).

Diode lasers operate at constant current or constant power mode. If the optical output power decreases below 80% of the specified output power or if the current increases by 20%, the end of the lifetime of this device has been reached. Operating current should be limited to derating rate $k_{current\%} = 75\%$ of maximum operating current. It is considered that such parameter will also limit the radiant output power from

Table 1
Specification of a 50 mW 1550 nm CW DFB Lasers with PM Fiber for WDM applications.

Limiting maximum rating parameters	Symbol	Min	Max	Unit
Laser diode				
Radiant output power from pigtail	P_{max}	–	100	mW
Forward current	I_F	–	600	mA
Storage temperature range	T_{stg}	−40	85	°C
Case operating temperature range	T_{op}	0	65	°C
Characteristic ($T_{chip} = T_\lambda$, $T_{amb} = 25$ °C, $P_0 = 50$ mW)				
Parameters	Symbol	Min	Max	Unit
Laser diode				
Radiant output power from pigtail @ 20 °C < T_λ < 35 °C	P_0	50	–	mW
Operating current	I_{op}	–	450	mA
Threshold current	I_{th}	–	40	mA
Central wavelength (ITU grid)	λ_c	1527	1610	nm
Laser set temperature for λ_c	T_λ	20	35	°C
Relative intensity noise @ 20–1000 MHz	RIN		−160	dB
Quantum efficiency	η_D	12 typ.		%
Thermoelectric cooler				
Cooler current	I_{cool}		1.5	A
Cooler voltage	V_{cool}		4.0	V
Reliability (Telecordia GR-468-CORE and MIL-STD-883).				
Long term wavelength drift	ML_λ	End Of Life: $\Delta\lambda = 0.2$ nm	300	Years
Activation energy	E_a	–	0.4	eV

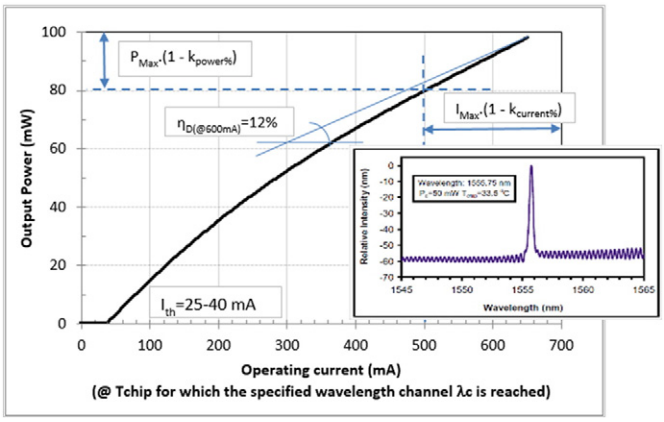

Fig. 2. Typical performance characteristics (P-I curve) of a 1550 nm DFB laser module from Manufacturer M.

pigtail. Assuming the threshold current I_{th} and the Differential Quantum Efficiency η_D, the radiant output power from pigtail will be limited to $k_{power\%}$ of maximum radiant output power ($P_{max\text{-}rating}$) referring to Fig. 2.

If Quantum Added Efficiency variation is in a statistical range values as observed from a manufacturing lot, derating parameter can change according to the following expression of current derating parameters calculated from maximum rating limits, Quantum Added Efficiency and derating on output power:

$$k_{current\%} = 1 - \frac{P_{max\_rating}}{I_{max\_rating}} \cdot \frac{(1 - k_{power\%})}{\eta_D(@I_{max\_rating})}. \quad (9)$$

As shown in Fig. 3:

For $\eta_D < 12\%$, derating is limited by power rating limit.
For $\eta_D > 12\%$, derating is limited by current rating limit.
For $\eta_D = 12\%$, derating is limited by power rating limit 50% and current rating limit 75%.

3.1. Numerical application for the determination of γ's

Considering the stress factors χ to be either the bias current I or the output power P(I), and knowing the reliability model described in the literature [29] are related to wearout failure as gradual degradation attributed to the growth of material defects, bulk failure results primarily from crystal defect in the region where high intracavity field circulates, Catastrophic Optical Mirror Damage (COMD). Elevated currents can bring out many of the degradation mechanisms associated with point defects in devices. If J is defined as the current density, the lifetime of the device is defined as t, and the empirical value parameter is defined as n, then there exists a relationship such that $t \approx I^{-m}$.

Similarly, the lifetime of laser diode varies inversely proportional to the power loading at the facet [30] and follows the power law $t \approx P^{-n}$.

The generic relations Eqs. (4.a) and (4.b) modeling the function stress factors for $i = 1$ to M, and bearing in mind the current and output power can be normalized w.r.t. their failure limits when burnout is reached can be defined as:

$$e^{-\nu_I \cdot \left(\frac{I}{I_{burnout}}\right)} = \gamma_I \left(\frac{I}{I_{burnout}}\right)^{-m} \text{ and } e^{-\nu_P \cdot \left(\frac{P}{P_{burnout}}\right)} = \gamma_P \left(\frac{P}{P_{burnout}}\right)^{-n} \quad (10)$$

assuming constants ν_I and ν_P to be determined experimentally. Eq. (6) becomes:

$$c(I,P) = 1 - \frac{k.T}{E_a} \cdot \nu_I \cdot \left(\frac{I}{I_{burnout}}\right) - \frac{k.T}{E_a} \cdot \nu_P \cdot \left(\frac{P}{P_{burnout}}\right). \quad (11)$$

Fig. 4 generalizes the BAZ model according to Eq. (11) showing the change of one electrical parameter, and so this drift is considered to describe the concept if this failure mode signature is proportional to the internal Free Energy of the laser diode.

With γ_I and γ_P are constants to be determined when applying the following boundary conditions (Eq. (11)):

Condition 1 (no stress): $I = 1\% \cdot I_{max\_rating}$, $P = 1\% P_{max\_rating}$, induces $c(1\% I_{max\_rating}, 1\% \cdot P_{max\_rating}) = 1$.
Condition 2 (derating limits): for $I = 75\% \cdot I_{max\_rating}$, $P = 50\%$. P_{max_rating}, leads to $c(75\% I_{max\_rating}, 50\% P_{max\_rating}) = c_0$.
Condition 3 (catastrophic failure at burnout limits): for $I = I_{burnout}$ and $P = P_{burnout}$ bearings to $c(I_{burnout}, P_{burnout}) = 0$.

Solving the system of 3 equations and 3 unknown parameters (ν_I, ν_P, c_0) established from these conditions and Eq. (8) we obtain for the considered laser diode module defined in Table 1 $\nu_I = 31.37$, $\nu_P = -31.70$ and $c_0 = 0.73$.

Using the following parameter values:
$T_{case} = 25$ °C, $I_{th} = 30$ mA, Ea = 0.6 eV, $\eta_D = 0.263$, $I_{max\_rating} = 600$ mA, $P_{max\_rating} = 150$ mW, Inom = 285 mA $I_{burnout} = 750$ mA, $P_{burnout} = 189.5$ mW, and Eq. (8), it is easy to plot showing the effective activation energy defined by Eq. (10) for any x and y in range [0, 1] and $T_{case} = 50$ °C. But considering Eq. (8), x and y parameters are linked and the final plot of effective activation energy is given in Fig. 5. As seen, the effective activation energy is reduced due to a joined function of stress factors applied showing how the BAZ model may reflect the physical impact of such multiple stresses as shown in Fig. 6.

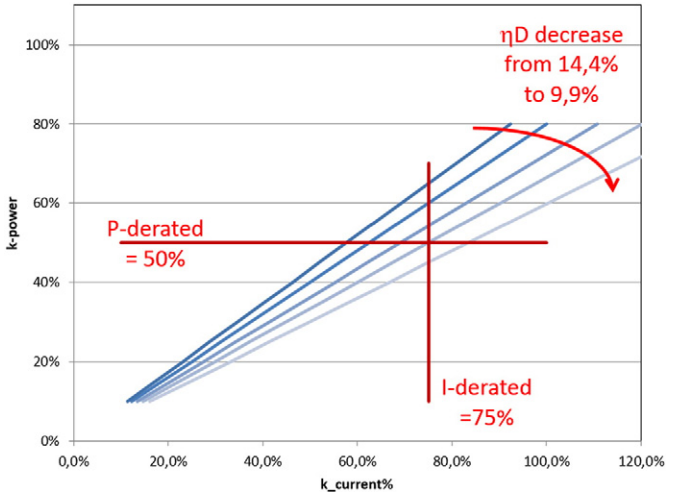

Fig. 3. Maximum rating limits and derating conditions (normalized w.r.t. maximum rating limits) required for high reliability application (effect of lot distribution due to lot Quantum Efficiency and threshold current dispersion).

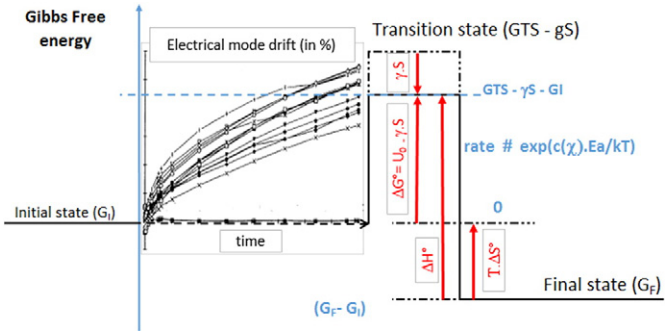

Fig. 4. Generalized BAZ model (Eq. (**11**)).

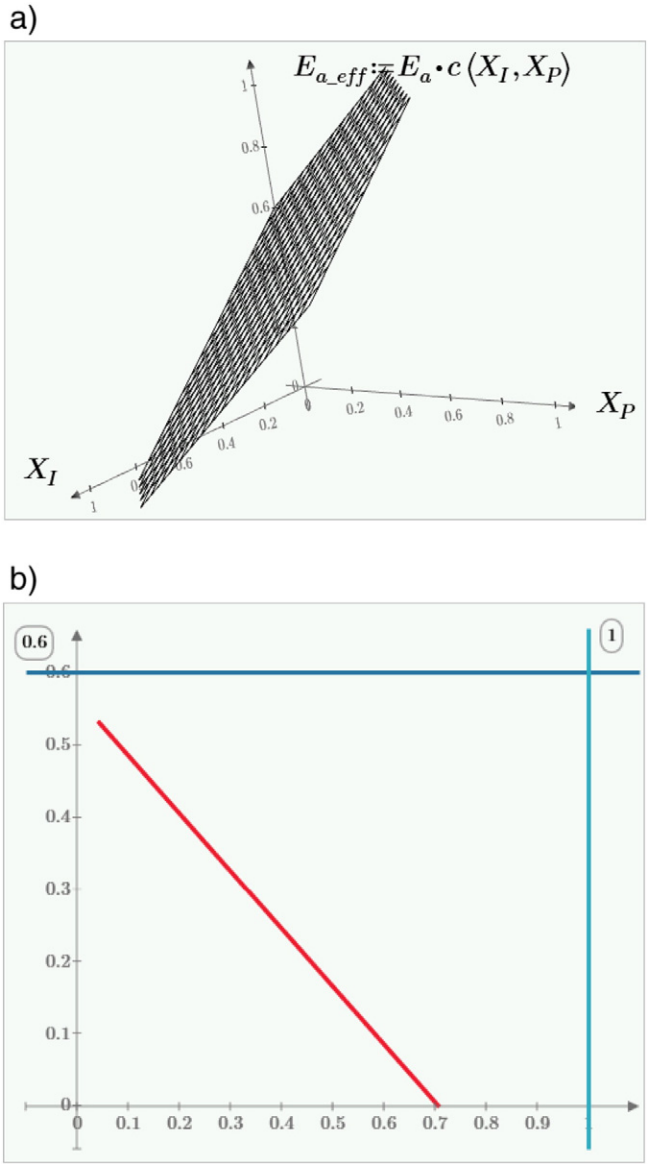

Fig. 5. a) Effective activation energy defined by Eq. (**10**) for $0 \le \chi_I \le 1$ and $0 \le \chi_P \le 1$. b) Effective activation energy defined by Eqs. (**10**) and (**8**) for $I_{th}/I_{burnout}$ ($0 \le \chi_I \le 1$).

One can note that the burnout limits are reduced when applied simultaneously and we can observe that the effective activation energy is reaching 0 for $x = I/I_{burnout} = 70\%$ i.e. before to reach the limit determined experimentally.

As a consequence maximum rating limits should be carefully established knowing this mechanisms and the related sequence of evaluation test sequence should be constructed accordingly as we will see now.

Recalling the derating parameters limits fixed by existing quality standards defined for space application. The derating parameters for optoelectronic devices are defined in Table 2 of ECSS-Q-ST-30-11C family-group code 18-01 to 18-05.

3.2. Discussion: How to establish an evaluation stress test program to consolidating a reliability model?

Considering laser module temperature for λc is defined at 35 °C maximum and case operating temperature range is fixed per data sheet to be 0 < Top < 85 °C, junction temperature Tj defined in accordance with

Table 2
Derating table of ECSS-Q-ST-30-11C family-group code 18-01 to 18-05.

Parameters	Load ratio or limit
Light emitting diode	
Forward current	Manufacturer recommended value, or derate to 50% if not available
Reverse voltage	Derate to 75%
Laser diode module	Derating rate defined at $T_{op} = T_{junction\_max}$
Forward operating current $I_{op\_derated}$	75% of maximum rating operating current (note 2)
Radiant output power from pigtail $P_{op\_derated}$	50% of maximum radiant output power from pigtail (note 2)
Junction temperature (T_j) imposed by TEC	85 °C or T_{j_max} − 40 °C (whichever is greater) (note 1)

Note 1: $T_{j\_max} = 85$ °C: This value to be validated from relevant evaluation and qualification test program.
Note 2: Derating to be applied on $I_{op\_derated}$ (75%) or on $P_{op\_derated}$ (50%) as per qualification.

ECSS-Q-ST-30-11 must be compliant to $Tj_{max} = 85$ °C for laser diodes or $Tj_{max} - 40$ °C whichever is lower,

- ✓ First step consists: to define a methodology for determining the key junction temperature parameter, and to assess and consolidate the thermal resistance measurement techniques.
- ✓ Second step: the maximum rating table and the specification limit parameters of laser diode module should be characterized over a temperature range extended to −20 °C, +85 °C when possible (this will depend on Thermoelectric cooler capability and maximum rating associated limits).
- ✓ Third step: assuming thermal resistance range, to confirm maximum junction temperature imposed by TEC, will not exceed $Tj_{max} = 85$ °C or $Tj_{max} - 40$ °C whichever is lower in order to allow Median life long term reliability at EOL (End-Of-Life) for criteria $\Delta\lambda = 0.2$ nm will be higher than 300 years.

Typical activation energy of such 1.55 μm DFB laser is correlated to diffusion phenomenon of interface defects between active zone and waveguide (Fig. 6). Degradation (nature and localization) of DFB-LD technology has been well described for example in Ref. [31] were the following failure mechanisms were recalled:

i. Intrinsic defects located between active and blocking layer (due to misfits or threading dislocations), induce an increase of threshold current I_{th}. While an increase of misfit concentration in active zone implies an increase of internal number of carriers injected in the active zone increasing the rate of non-radiative recombination in active area.
ii. Electrostatic discharges (Typical failures for ESD voltage around 200 V), are bringing defects located between passive and active

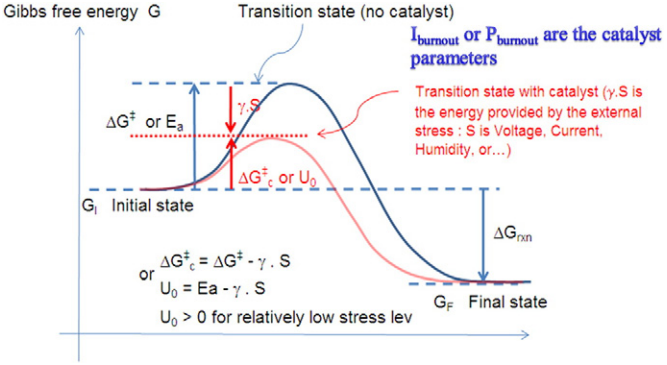

Fig. 6. Suggested TST applied to reliability of DFB laser diode module.

zone associated to non-uniform overgrowth of p-InP and when located on the active region induces catastrophic central wavelength deviation (1 nm) for forward ESD stresses. Crystal damages can occur depending on the amplitude of the ESD bias. Crystal misfits related to ESD are generally observed by an increase of leakage current. Current leakage paths may result in an increased threshold current reducing quantum efficiency and central wavelength drift.

iii. Failure on passive waveguide also called spot-size converter. Hetero-interface between active zone and passive waveguide could be filled of defects responsible to photon absorption allowing explaining optical power losses.

A reliability test program sequence is under construction in the frame of the industrialization and the space validation of a new 1.55 μm DFB laser diode module supported by the European Component Initiative under ESA-ESTEC contract n° 4000110310 and has been predefined according to the following recommendations.

Stage 1 will be related to initial performance purpose: To characterize laser diode lot in chip form and at module level after screening including L(I) plots for junction temperature range 10 °C to 90 °C (each 20 °C), I range up to 75% of maximum rating, I(V) (forward) plots in semic-log plots for injection current range from 10–9 A to I_{max} at 3 junction temperatures I(V) reverse V range −2 V, 0 V (@ $T_{junction}$ = 20 °C) and determination of the Normal distribution plots (complete lot) for main parameters (@ $T_{junction}$ = 20 °C): I_{th}, η_D, central wavelength characteristics (@Tj = 20 °C), RIN (@ 375 mA, frequency range). Characterization of burnout failure conditions for high current drive $I_{burnout}$ at chip and module level (@ $T_{junction}$ = 20 °C) and related COMD failure or/and black line (increase of the drift of optical power and leakage current I(V) plot in log–log scale at low injection current).

Stage 2 is dealing with the determination of the activation energy E_a based on high temp storage test sequence at 3 temperatures: this is the baseline of the BAZ model (to use chip on carrier for simplify measurement).

Stage 3: to perform step stress sequence to help defining endurance life test sequences

Stage 4: To perform endurance life test sequences to consolidate the determination of γ's based on the described model and related to the given stress factors:

a) current bias (DC and pulse)
b) and/or for Output Power
c) and/or for radiation $\gamma_{radiation}$,

Stage 5: Perform step stress tests in order to increase number of devices up to 15 + 2 CD. To clarify T_{case} and $T_{junction}$ (not to stress TEC).

Stage 6: To define a Design of Experiment (DoE) for accelerated endurance test sequence at 3 temperatures and 3 biasing conditions applying constant current and constant output power in order to determine the γ's. The biasing conditions will be consolidated from step stress tests in order to get more than 50% failure in a short period of time (typically close to 1000 h).

4. Conclusion

The activity presented in this paper is a study conducted under the European Component Initiative program funded by European Space Agency. The objectives are to design, develop, manufacture and space validate a DFB Laser Module at 1.55 μm manufactured by a European supplier.

The paper has proposed a generalized view of the existing reliability model named Boltzmann–Arrhenius–Zhurkov model. The definition of maximum rating and derating parameters have been extracted and justified thanks to the model presented. Reliability figures including activation energies and accelerating factors related to the three main parameters were commented (temperature, current and output optical stress). It has been shown how these multiple stresses interact and modify the effective activation energy. Additional evaluation step stress program was suggested to consolidate and validate the model.

The Transition-State Theory was used formerly to model the Probabilistic Design for Reliability (PDfR) concept developed for electronics devices in harsh environment and adapted to the specific case of a 1.55 μm DFB laser module.

The equivalence with Transition State Theory is supported by the fact that the transition rate is similarly outlined by equation of BAZ model when a catalyst effect is invoked.

A numerical application for the determination of γ's was explained and provides a support to propose a discussion to establish an evaluation stress test program for consolidating a reliability model of this type of product.

Such a reliability test program sequence is now under construction in the frame of the industrialization and the space validation of a new 1.55 μm DFB laser diode module supported by the European Component Initiative under ESA-ESTEC and has been predefined.

Acknowledgment

Authors gratefully acknowledge the European Space Agency for supporting this study contract n°4000110310.

References

[1] D.G. Truhlar, B.C. Garrett, S.J. Klippenstein, Current status of transition-state theory, J. Phys. Chem. 100 (31) (1996) 12771–12800.
[2] G.S. Hammond, A correlation of reaction rates, J. Am. Chem. Soc. 77 (1955) 334–338, http://dx.doi.org/10.1021/ja01607a027.
[3] E. Suhir, "Predicted Reliability of Aerospace Electronics: Application of Two Advanced Probabilistic Concepts", IEEE Aerospace Conference, March 2-9, 2013, Big Sky, Montana, Paper 2037, 2013.
[4] A. Bensoussan, E. Suhir, Design-for-reliability (DfR) of aerospace electronics: attributes and challenges, IEEE Aerospace Conference, March 2–9, 2013, Big Sky, Montana, Paper 2057, 2013.
[5] J.R. Black, Electromigration — a brief survey and some recent results, IEEE Trans. ED, ED-16, 3881969.
[6] H. Eyring, S. Lin, Basic Chemical Kinetics, Wiley&Sons, 1980.
[7] B.N. Agarwala, et al., Dependence of electromigration-induced failure time on length and width of aluminum thin-film conductors, J. Appl. Phys. 41 (1970) 3954, http://dx.doi.org/10.1063/1.1658395.
[8] D.S. Pect, "Comprensive model for humidity testing correlation", Proc. 24th IEEE IRPS (1985) 44–50.
[9] Final report California Institute of Technology Jet Propulsion Laboratory Pasadena, California, Hydrogen Effects on GaAs Microwave Semiconductors, July 1997 (report N°: SMC97-0701).
[10] S. Kayali, et al., GaAs MMIC Reliability Assurance Guidelines for Space Applications, vol. 96-25, JPL Publication, December 15, 1996.
[11] E. Wigner, The transition state method, Trans. Faraday Soc. 34 (1938) 29–41.
[12] M. Evans, M. Polanyi, Inertia and driving force of chemical reaction, Trans. Faraday Soc. 34 (1938) 11–29.
[13] A. Christou (Ed.), Reliability of Gallium Arsenide MMIC, John Wiley & Sons, 1992 (Calce Electronic Packaging Research Center, University of Maryland, USA).
[14] H. Cui, Accelerated Temperature Cycle Test and Coffin–Manson Model for Electric Packaging, RAMS, 2005.
[15] I.C. Chen, et al., A Quantitative Physical Model for TDDB in SiO_2, Proc. IRPS, 23 1985, p. 24.
[16] I.C. Chen, et al., Accelerated testing of TDDB in SiO_2, IEEE ED Letters, EDL-8, 1401987.
[17] Mingzhi Dai, et al., A model with temperature-dependent exponent for HCI in high-volatge nMOSFETs involving hot-hole injection and dispersion, IEEE Trans. Electron Devices 55 (5) (May 2008) 1255–1258.
[18] E. Takeda, et al., New hot-carrier injection and device degradation in submicron MOSFETs, Solid State Electron Devices IEE Proc. I 130 (3) (June 1983) 144–150.
[19] K. Decker, GaAs MMIC Hydrogen Degradation Study, GaAs Reliability Workshop Digest, 1994.
[20] W. Roesch, Accelerated effects of hydrogen on GaAs MESFETs, GaAs Reliability Workshop Digest, 1994.
[21] M.J. Delaney, et al., Reliability of 0.25 μm GaAs MESFET MMIC process: results of accelerated lifetests and hydrogen exposure, GaAs Reliability Workshop, 1994.
[22] M. Ciappa, et al., Lifetime Modeling of Thermomechanics Related Failure Mechanisms in HP IGBT Modules for Traction Applications, ISPSD, Cambridge, UK, April 2003.
[23] Dieter K. Schroder, et al., Negative bias temperature instability: road to cross in deep submicron silicon semiconductor manufacturing, J. Appl. Phys. 94 (1) (July 2003).

[24] S. Glasstone, K.J. Laidler, H. Eyring, The Theory of Rate Processes: the Kinetics of Chemical Reactions, Viscosity, Diffusion and Electrochemical Phenomena, McGraw-Hill, New York, 1941.
[25] M.N. Yoder, Ohmic contacts in GaAs, Solid State Electron. 23 (1980) 117–119.
[26] C.P. Lee, B.M. Welch, W.P. Fleming, Reliability of AuGe/Pt and AuGe/Ni ohmic contacts on GaAs, Electron. Lett. 17 (1981) 407–408.
[27] Bensoussan, et al., "Reliability of a GaAs MMIC Process Based on 0.5 μm Au/Pd-Ti gate MESFETs", 32th Annual proceedings Reliability Physics, San Jose, CA, (April 12-14, 1994) 434–445.
[29] H. Hemmati, Near-Earth Laser Communications, in: H. Hemmati (Ed.) CRC press Taylor & Francis Group, Pasadena, Californa, 2009.
[30] M. Krainak, et al., Performance tests of Quasi-CW diode Pump Arrays conducted or sponsored by NASA Goddard Space Flight Center, 1997 Digest of LEOS Summer Topical Meetings: Advanced Semiconductor Lasers and Applications, Montreal, Quebec, Canada, Aug. 11–15 1997.
[31] Y. Deshayes, et al., 'Estimation of lifetime distributions on 1550 nm DFB laser diodes using Monte-Carlo statistic computations", in: Hans G. Limberger, M. John Matthewson (Eds.), Reliability of Optical Fiber Components, Devices, Systems, and Networks II, Proc. of SPIE, Vol. 5465, April 2014.